Cosmic Ray Tests of a 4.6m-long Test Drift Chamber for JLC

Y.Kurihara[a], *A.Yamaguchi*[b], *S.Sudo*[b], *T.Abe*[c1], *K.Fujii*[a], *N.Ishihara*[a], *N.Khalatyan*[a], *T.Matsui*[a], *O.Nitoh*[b], *T.Ohama*[a], *H.Okuno*[a], *A.Sugiyama*[c], *K.Takahashi*[b], *T.Watanabe*[d], *T.Yoshida*[a],

[a] High Energy Accelerator Research Organization(KEK), Tsukuba, 305-0801, Japan
[b]Tokyo University of Agriculture and Technology, Tokyo 184-8588, Japan
[c]Department of Physics, Nagoya University, Nagoya 464-8602, Japan
[d]Kogakuin University, Tokyo 163-8677, Japan

Abstract

Performance of a 4.6 m-long drift chamber filled with a CO_2 iso-butane (90 : 10) mixture was studied using cosmic ray data, in the course of detector R&D for JLC. After correcting the data for wire displacements due to gravitational and electrostatic forces, a spatical resolution of 100 μm per wire was achieved over the full length of the chamber. The relation between wire efficiency and oxygen remnant in the chamber gas is also discussed.

[1]Now at SLAC, California, USA

1 Introduction

One of the most important goals of experiments at a future linear e^+e^- collider such as JLC[1] is to discover and study the Higgs boson. In particular, if one wants to confirm the narrowness of the Higgs boson by measuring the distribution of the recoil mass opposite to the lepton pair from the Z^0 boson decay in the process $e^+e^- \rightarrow H^0Z^0$, the recoil mass resolution should at least be as good as the beam energy spread of the collider. This requires a high resolution central tracker with a momentum resolution of $\sigma_{p_T}/p_T \sim 10^{-4} \times p_T(\mathrm{GeV})$. Such a tracking chamber becomes as large as 2.3 m in radius, even if we assume 100 sampling points with a spatial resolution of 100μm per wire in a magnetic field of as high as 2 T. In addition, to ensure this momentum resolution over a polar angle range of $45^\circ < \theta < 135^\circ$, the chamber has to be as long as 4.6 m. Due to substantial gravitational and electrostatic sags, achieving a spatial resolution of 100 μm/wire for a 4.6 m-long chamber is quite non-trivial.

In order to investigate potential difficulties inherent in such a long drift chamber, we constructed a 4.6 m-long test chamber and a precision optical survey system for wire positions. We then compared measured and calculated wire sags and found a good agreement as reported in [3]. We thus established a method to predict wire positions for given wire and high voltage configurations. The remaining question is whether we can actually achieve the required spatical resolution over the full length of the 4.6 m-long chamber, armed with the quantitative knowledge on the wire sags. In order to confirm this, we studied the performance of the test chamber using cosmic rays. In this report, we describe results from the cosmic-ray tests of the 4.6 m-long test chamber: the spatial resolution and efficiency for each sense wire, and their dependence on the incident position and angle of a cosmic ray particle. The effects of the oxygen remnant in the chamber gas volume is also discussed.

2 Test Chamber Parameters

In order to fulfill the physics requirements, we need to achieve the following performance goals: $\sigma_{r\phi} \simeq 100$ μm, $\sigma_{rz} \simeq 1$ mm, and and two-track separation better than 2 mm, in a magnetic field of 2 T and for a wire length of 4.6 m. The second and the third of the above goals are to ensure good track-cluster matching in a jetty environment. One possible approach to realizing these design goals is to use a slow gas mixture with a small Lorenz angle and a mini-jet cell structure to allow stereo wires for z-coordinate measurements. We designed such a mini-jet cell so as to realize the design goals. The current cell design is shown in Fig. 1-(a) which also specifies our wire naming convention to be used hereafter. The cell has 5 sense wires ($S1$ to $S5$) held at 2.5 kV and spaced 1 cm, with each surrounded by ground wires ($G1$ to $G6$) in the sense wire plane and grid wires ($GL1$ to $GL6$ and $GR1$ to $GR6$) at -0.5 kV placed 5 mm away from it. The two dummy sense wires ($D1$ and $D2$) at the both ends of the sense wire plane are held at 2.15 kV and stabilize the upper- and the lower-most sense wires ($S1$ and $S5$). The maximum drift length is 5 cm where the drift field is produced by 10 field shaping wires ($F1**$ to $F10**$)

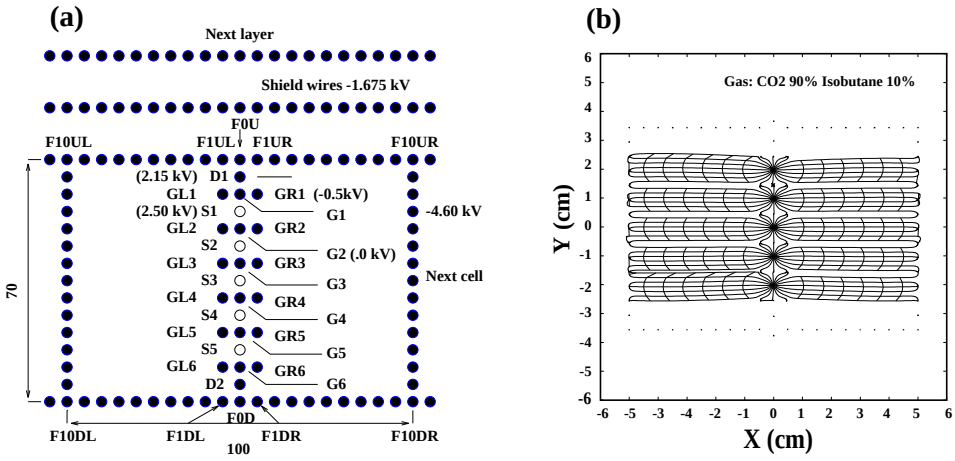

Figure 1: (a) possible mini-jet cell structure and (b) corresponding drift lines.

whose potentials change linearly in this order from -0.5 kV to -4.6 kV, and by left and right edge field wires held at -4.6 kV. The wire diameter is 30 μm for sense wires and 125 μm for the others. The high voltages on the wires were chosen so as to get as uniform a drift field as possible with minimum electrostatic forces, while keeping a reasonable gas gain for a chamber gas mixture of 90% CO_2 and 10% iso-butane. Fig. 1-(b) plots the drift lines calculated with a drift chamber simulation program GARFIELD [2].

Our 4.6 m-long test chamber has seven identical cells with the cell parameters described above. The layout of the seven cells is shown in Fig. 2. In what follows, we are

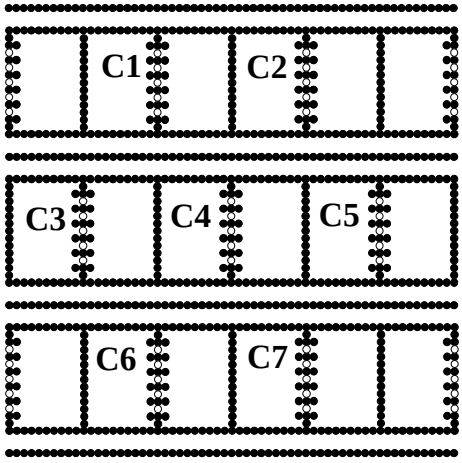

Figure 2: Cell layout of our 4.6 m-long test chamber.

going to deal with wires belong to the central cell ($C4$), since they are the only wires equipped with readout electronics.

Before stringing wires, we surveyed the end-plates to check their machining precision and found that the standard deviation of the actual wire hole positions from the nominal ones to be less than 8.2 μm. The sense wires are gold-plated tungsten and all the other

wires are gold-plated aluminum. The reason for this choice of Al as the wire material is to minimize the total wire tension so as to reduce the thickness of the chamber end-plates as required by end-cap calorimeters. The wire stringing took us three weeks.

3 Experimental Setup

3.a Gas System

Our test chamber is filled with a gas mixture of 90%CO_2 and 10% iso-butane, which is a so called *'cool gas'* having a small enough diffusion coefficient to keep a good spatial resolution over the full drift length of 5 cm for our current cell design. High purity CO_2 (99.99%) and iso-butane (99.98%) gases are supplied to the test chamber through an oxygen filter. Their flow rates are stabilized at 450 and 50 cc/min, respectively, by a set of mass flow controllers calibrated for these gases. The oxygen concentration is monitored at the outlet by an oxygen monitor. The oxygen remnant in the chamber was around 60 ppm throughout the cosmic ray tests, unless intentionally increased for a test purpose. The gas pressure in the test chamber is determined by a bubbler and is slightly higher than the atmospheric pressure.

3.b Trigger System

Cosmic rays passing through the test chamber were triggered by two plastic scintillation counters sandwiching the chamber's sense volume (see Fig.3). These two trigger counters are idential and each of them has an acceptance of 20 cm $\times$ 20 cm, being big enough to cover the full sense volume of the central cell ($C4$). In order to study the position and incident angle dependences of the chamber performance, these trigger counters were moved accordingly. These trigger counters also provided a common stop signal to our flash-ADC described below.

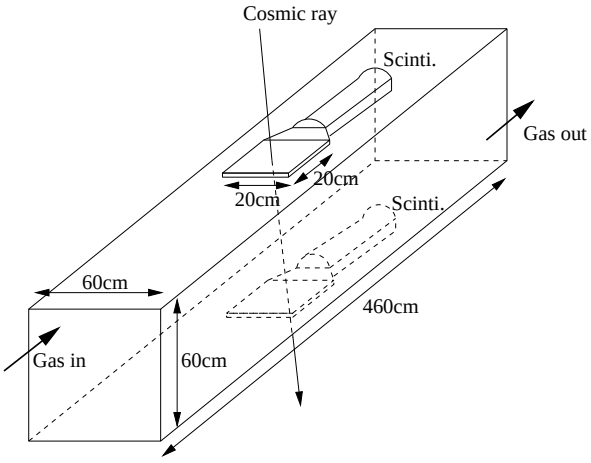

Figure 3: Experimental setup.

3.c Data Acquisition

A chamber signal is first amplified by a pre-amplifier, which is mounted on an end-plate of the test chamber, and by a post-amplifier after passing through a 5 m-long twisted pair cable. The gain of the pre-amplifier is about 200 mV/pC for the short pulse. The signal from the post-amplifier is fed to an 8-bit flash-ADC (REPIC RPC-250), which has a 500 MHz sampling frequency over a 1.6 μsec time window. Any pulse from 0 to -1 V is chopped into 2 nsec time slots and converted to a train of digits in the interval of 255 to 0 counts by this flash-ADC. The overall gain was adjusted so as to give a maximum amplitude of around 100 at the peak of a typical pulse. The pulse shapes for a typical cosmic-ray track is shown in Fig.4. This flash-ADC fully covers the maximum drift time of the test chamber (about 600 μsec) and provides a high enough sampling frequency to ensure a good enough resolution (2 nsec corresponding to 16 μm drift equivalent). The digitized pulse form is read out and recorded on a disk by a computer (NEC PC98) through a CAMAC system.

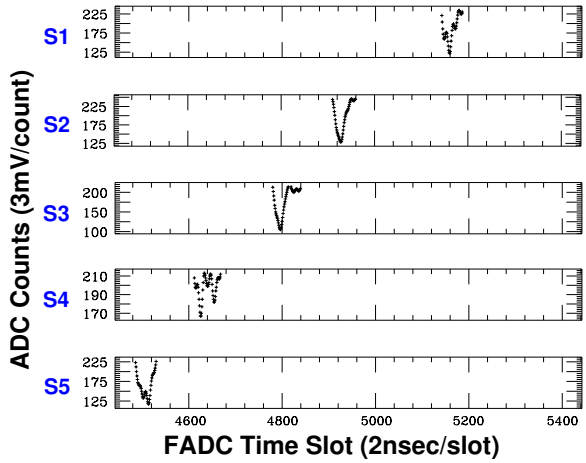

Figure 4: Pulse shapes for a typical cosmic-ray track.

4 Analysis

4.a T_0 Determination and x-t Relation

Any pulse which continues longer than 120 nsec above the threshold (pedestal+3 counts) was regarded as a signal pulse. The arrival time of the signal pulse was determined by its leading edge at which the pulse height exceeded the threshold. The so called T_0 (the signal arrival time for zero-length drift) was decided as the shorter-drift-length edge of the arrival time distribution for each sense wire. The drift time (t) can then be defined as the arrival time measured from T_0. To convert the drift time to the drift length, we use the x-t relation calculated with GARFIELD for each wire. The validity of the calculated x-t relation was experimentally confirmed by compareing the drift velocity

given by GARFIELD with independent drift velocity measurements[4]. The x-t relation is shown in Fig.5 for the central sense wire ($S3$).

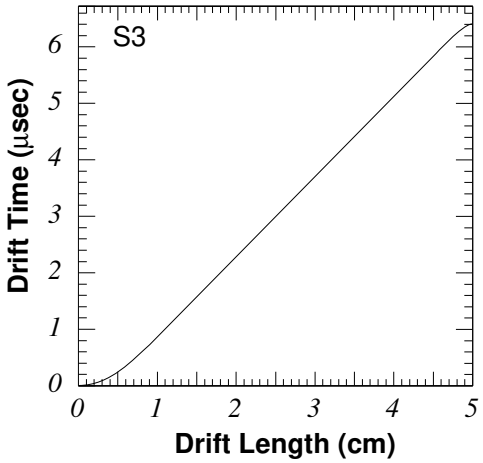

Figure 5: x-t relation calcuated with GARFIELD for the central sense wire of our test chamber.

4.b Reference Track Selection

When more than four out of the five sense wires in the central cell have the above-defined signal pulses, we regard the event as having a track candidate. This preselection is necessary since the trigger counters sandwiching the chamber are twice as wide as the central cell and, consequently, there are events with no tracks in the central cell ($C4$).

In order to study the efficiencies and spatial resolutions of individual sense wires, we need to use events with a well defined reference track consisting of four hits on the wires excluding the wire to study. Such a track was selected by demanding the following conditions:

- χ^2 of the linear fitting to the four hits had to be less than 40.
- There had to be no left-right ambiguity.
- The expected hit position for the wire in question had to be well within the fiducial volume of the cell.
- The four signal pulses that defined the track candidate had to be within 500 μm from the fitted track.

4.c Wire Alignment

The sense wires are nominally aligned in the straight line dividing the drift cell into two at the center. Any small deviations from the nominal positions may, however, act as a seed for much enhanced displacements of the sense wires in the middle due to electrostatic force. The sense wire positions had been precisely mapped out by a direct optical survey[3]. The

survey also confirmed the stability of the sense wires against the turning on and off of the wire high voltages. The displacement pattern appears in the residual distributions for five-wire fits as the finite offsets (average residuals) as seen in Fig.6-(a). The hit

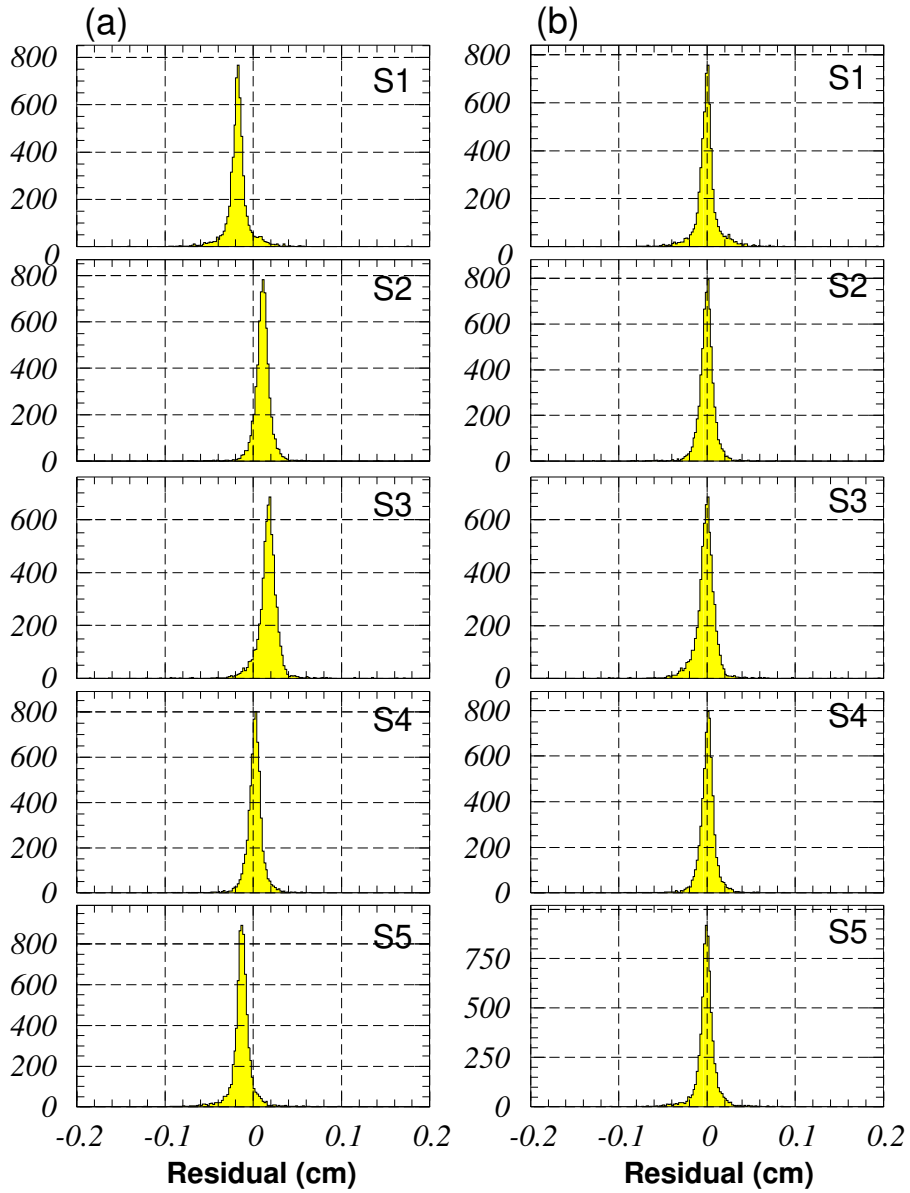

Figure 6: Residual distributions for 5-wire fits: (a) before and (b) after wire alignment.

positions were corrected for the offsets to make the residual distributions centered at zero (see Fig.6-(b)). We found the amount of the correction consistent with the direct optical survey.

5 Chamber Performance

5.a Spatial Resolution

With the reference tracks selected and the wires aligned, we can now calculate, on an event-by-event basis, the residual of each hit on the wire to look at as the distance from the reference track consisting of the four hits as defined above. The so-obtained residual distribution for the central wire ($S3$) is plotted in Fig. 7-(a) against the drift length for tacks passing through the central cell ($C4$) in the middle of the wires, with the two trigger counters vertically aligned so as to primarily sample tracks perpendicular to the sense wires. Fig. 7 shows the one-standard-deviation (1-σ) width of the residual distribution as

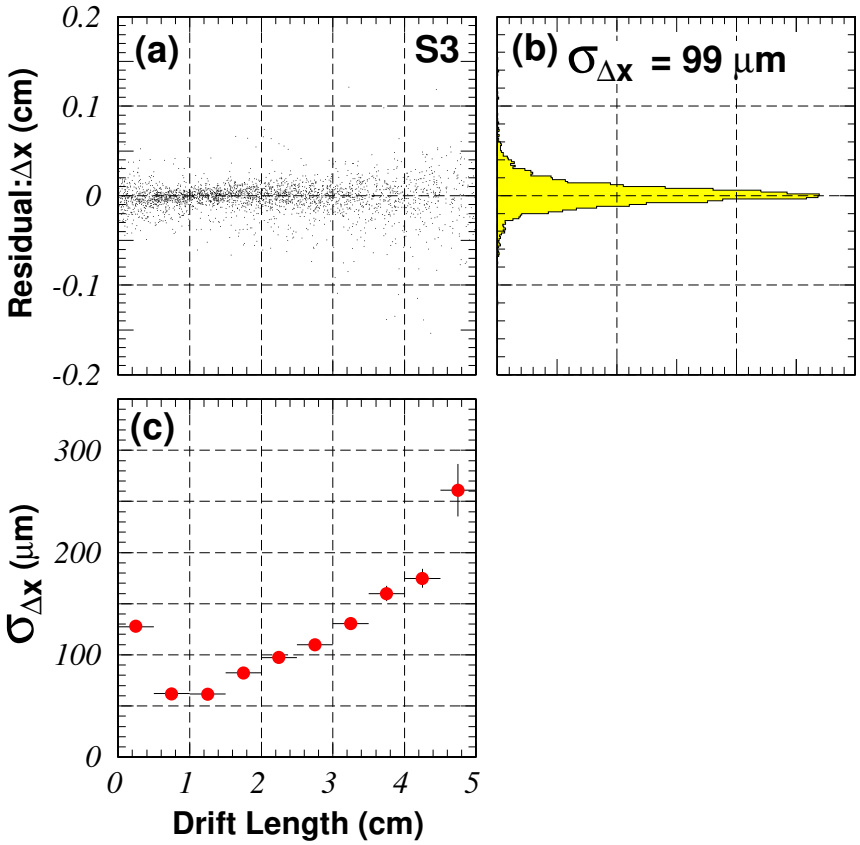

Figure 7: Residual for $S3$ at the center of the test chamber (a) plotted against drift length, (b) its projection to the vertical axis, and (c) the standard deviation of the residual distribution as a function of the drift length.

a function of the drift distance. The width is less than 100 μm for a drift length less than 2.5 cm, except for the vicinity of the sense wire[2]. It becomes, however, gradually worse

[2]The apparent degradation of the resolution near the sense wire is not only coming from primary ionization statistics but also from left-right ambiguity.

up to about 200 μm towards the edge of the drift volume. Fig. 7-(b) is the projection to the vertical (residual) axis, demostrating the overall residual distribution. The edge wires ($S1$ and $S5$) have wider distributions. This is due to the reference track extrapolation error for $S1$ and $S5$ being much larger than the interpolation error for $S2$ to $S4$. In order to estimate the intrinsic spatial resolution of each wire we calculated the track error as a function of the drift distance and subtracted it in quadrature on a bin-by-bin basis. We then averaged the resultant resolution over the drift distance to compensate the acceptance non-uniformity. The so-obtained overall intrinsic spatial resolutions for individual sense wires are summarized in Table 1. Inspection of the table tells us that the overall resolutions are around 100μm, satisfying our performance goal at least locally. A similar analysis was carried out for tracks passing though the central cell near the both ends of the wires, in order to make sure that the performance goal be satisfied over the full length of the chamber. Though the spatial resolutions became slightly worse, they are still close to 100 μm as listed in Table 1.

Table 1: Summary of spatial resolutions

Wire Number	Center	Ends	Inclined
S1	$117 \pm 19(\mu m)$	$130 \pm 70(\mu m)$	$114 \pm 41(\mu m)$
S2	$96 \pm 10(\mu m)$	$104 \pm 34(\mu m)$	$94 \pm 25(\mu m)$
S3	$107 \pm 12(\mu m)$	$142 \pm 37(\mu m)$	$95 \pm 19(\mu m)$
S4	$107 \pm 12(\mu m)$	$118 \pm 64(\mu m)$	$89 \pm 12(\mu m)$
S5	$133 \pm 61(\mu m)$	$174 \pm 61(\mu m)$	$94 \pm 25(\mu m)$

The intrinsic resolutions may also depend upon the incident angle of a track to the sense wires. In order to investigate this effect, we set the two trigger counters in the middle of the chamber but slightly displaced so as to primarily sample inclined tracks having an incident angle of around 45° to the wires. This incident angle (45°) corresponds to the maximum dip angle with the full number of sense wires for our current design of the JLC central tracker. The residual distribution for the central sinse wire ($S3$) is histogrammed in Fig. 8. The width of the residual distributions were translated into overall intrinsic spatial resolutions after the track error and acceptance corrections, and are summarized in Table 1. We thus confirmed that a spatial resolution of about 100μm up to an incident angle of 45°.

5.b Wire Efficiency

The efficiency for each wire was calculated as a function of the drift distance to be the fraction of tracks with actual hits on the wire in a 5-σ window. Fig. 9 is the results of the calculations, for an oxygen contamination in the chamber gas of about 60 ppm. The efficiency stays flat above 95% except in the last several bins close to the edge of the drift volume. The slight drop towards the edge is primarily coming from the track electron absorption due to the oxygen contamination.

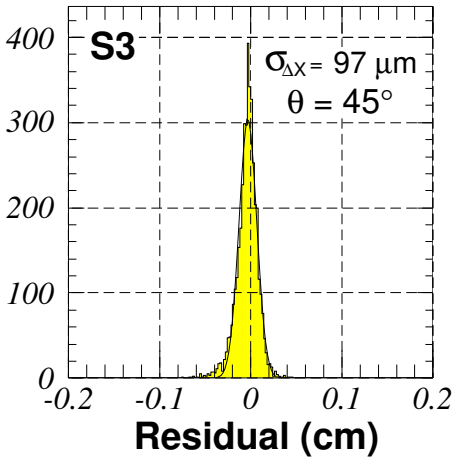

Figure 8: Same as Fig. 7-(b) but for an incident angle of 45° to the sense wire.

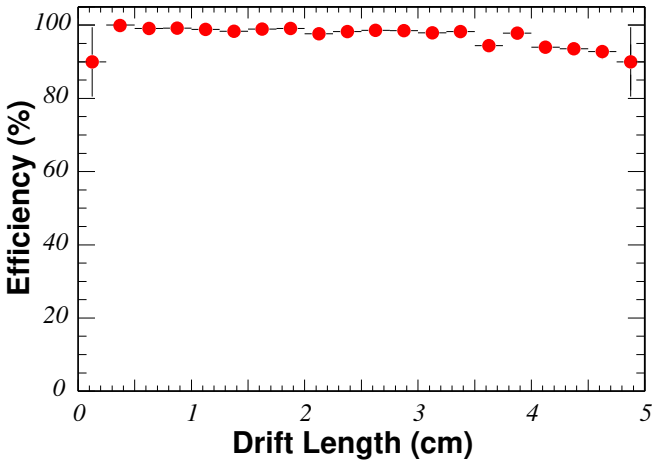

Figure 9: Efficiency of the central sense wire ($S3$) as a function of the drift distance.

5.c Effects of Residual Oxygen Gas

To investigate the effect of the oxygen contamination in the chamber gas, we compared the chamber performance for two different oxygen contaminations, 60 ppm and 120 ppm. The oxygen molecules, being electro-negative, capture some track electrons drifting towards a sense wire and make the signal pulse smaller as the drift length gets longer. We chose the chamber gas with a slow drift velocity to reduce the effect of the diffusion of the track electron clusters. This choice made the chamber more sensitive to a small contamination from electro-negative gases. The pulse height becomes smaller with the drift distance due to the diffusion. However, the total charge of the pulse must stay the same, as long as there is no track electron loss.

Plotted in Fig. 10-(a) is the integrated signal charge on $S3$ against the drift distance for an oxygen contamination of 60 ppm. The signal charge gets smaller as the drift distance becomes longer, indicating that an electro-negative gas at work.

In order to confirm this effect, we intenstionally increased the oxygen contamination to 120 ppm and measured the drift-length dependence of the signal charge. As seen in Fig. 10-(b), the pulse charge rapidly decreases with the drift distance and vanishes down below the threshold at the large drift distance, suggesting a total loss of track electrons.

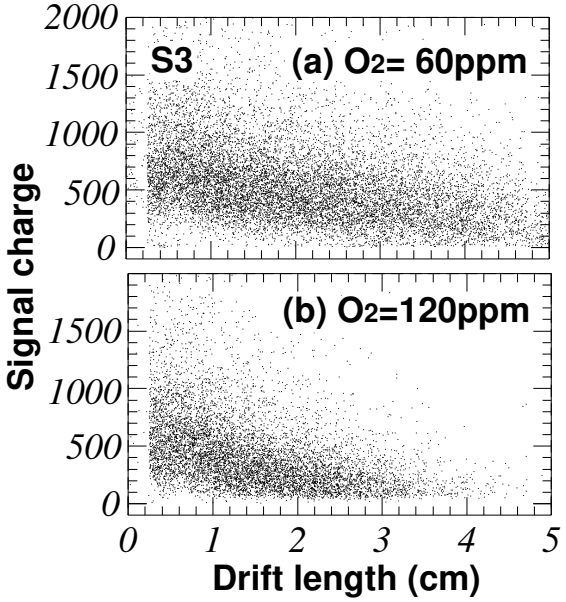

Figure 10: (a) Pulse charge on the central sense wire ($S3$) as a function of the drift distance for an oxygen contamination of 60 ppm. (b) Same as (a) but for an oxygen contamination of 120 ppm.

This effect not only diminishes the wire efficiencies but may also deteriorate the spatial resolutions in the large drift-length region. As a matter of fact, Fig. 7 shows a resolution increment with the drift distance larger than naively expected from diffusion. It may be explained by the track electron loss due to the oxygen contamination. A better performance can thus be expected if the oxygen contamination will be reduced.

6 Conclusions

We have constructed a 4.6 m-long test drift chamber in the course of JLC detector R&D's. The test chamber has the same wire length, cell structure, and chamber gas (CO_2 isobutane(90 : 10)) as a current design of the JLC central drift chamber. The performance of the chamber was studied by using cosmic ray events. It is confirmed that the test chamber satisfies the required spatial resolution of 100 μm per wire in the r-ϕ plane over the full length of the chamber for an incident angle of 0 to 45° to the wires even with a relatively high oxygen contamination. A better performance can be expected with gas system improvements.

References

[1] JLC group, KEK Report 92-16, December,1992.

[2] Veen Hove, A Drift Chamber simulation program GARFIELD, 1994.

[3] S. Sudou, N. Khalatyan, Y. Kurihara, T. Abe, K. Fujii, A. Sugiyama, K. Takahashi, T. Watanabe, Nucl. Instrum. Methods, A383 (1996) 391.

[4] A. Yamaguchi, Masters' Thesis (1998) 70, in Japanese.